Inorganic Chemistry

Communication

pubs.acs.org/IC

# Rearrangement of a Krebs-Type Polyoxometalate upon Coordination of N,O-Bis(bidentate) Ligands

Beñat Artetxe,[†] Santiago Reinoso,*[,†] Leire San Felices,[‡] Luis Lezama,[†,§] Aroa Pache,[†] Cristian Vicent,[∥] and Juan M. Gutiérrez-Zorrilla*[,†,§]

[†]Departamento de Química Inorgánica, Facultad de Ciencia y Tecnología and [‡]Servicios Generales de Investigación SGIker, Facultad de Ciencia y Tecnología, Universidad del País Vasco UPV/EHU, P.O. Box 644, 48080 Bilbao, Spain

[§]BCMaterials, Parque Científico y Tecnológico de Bizkaia, Edificio 500−1, 48160 Derio, Spain

[∥]Serveis Centrals d'Instrumentació Científica, Universitat Jaume I, Av. Sos Baynat s/n, 12071 Castellón de la Plana, Spain

Supporting Information

**ABSTRACT:** Selective coordination of 2,3-pyzdc to the Krebs-type $[\{Ni(H_2O)_3\}_2(WO_2)_2(SbW_9O_{33})_2]^{10-}$ anion promotes a skeletal rearrangement that results in the $[(2,3\text{-pyzdc})_2\{NaNi_2(H_2O)_4Sb_2W_{20}O_{70}\}_2]^{22-}$ (**Ni$_4$**) hybrid dimer showing a novel dinickel containing a 20-tungsto-2-antimonate(III) framework stabilized by N,O-bis-(bidentate) bridging ligands. The solution stability and magnetism of **Ni$_4$** is discussed.

The organic derivatization of polyoxometalates (POMs) constitutes a current hot topic within the chemistry of this well-known family of anionic metal−oxygen clusters with a unique variety of structures and potential applications (e.g., catalysis, medicine, materials science).[1] The covalent attachment of functional organic groups to POM skeletons can confer new properties on the resulting hybrid species and allow the firm immobilization of these clusters on diverse surfaces to construct new composite materials and devices.[2] Among the different synthetic approaches for designing such a type of hybrid POMs, the combination of lacunary polyoxotungstates with p-block organoderivatives or the replacement of O atoms in the POM shell with O- or N-donor ligands like trisalkoxo or organoimido groups can be cited as two of the most relevant. Highly elaborate organic functionalities have also been achieved via postfunctionalization reactions involving further multistep synthetic work on these hybrid POM platforms.[3]

An alternative route for preparing hybrid POM species consists in performing classical coordination chemistry on suitable d- or f-metal substituted clusters with exposed metal centers showing coordinated labile molecules (e.g., water) that are accessible for being replaced with organic ligands. Steric hindrance and electronic repulsion between anionic ligands and POMs often make complexation of these centers challenging, but the combination of polydentate ligands and POM assemblies with multiple coordination sites in close vicinity has proven to enhance this strategy.[4] In this context, we recently explored the potential of Krebs-type $[\{M(H_2O)_3\}_2(WO_2)_2(SbW_9O_{33})_2]^{10-}$ POMs (**M$_2$Sb$_2$**) as precursors in ligand replacement reactions. This class of sandwich anions offers several advantages for such reactions, like (i) containing six accessible water molecules, (ii) being stable in solution in a wide pH range, and (iii) showing a structure that allows systematic compositional variations.[5] We demonstrated that functionalization is highly dependent on the specific nature of the ligand by reporting a series of seven $[\{ML(H_2O)\}_2(WO_2)_2(SbW_9O_{33})_2]^{12-}$ hybrid species, which represent the first organic derivatives of 3d-metal-disubstituted Krebs-type POMs and where L accounts for N,O-chelating carboxylate derivatives of aromatic N-heterocycles.[6]

Now, we are interested in extending our studies to a wider range of ligands, especially to those with the ability to arrange POM clusters in extended assemblies. On the basis of our previous work, we focused our attention on planar N,O-bis(bidentate) linkers and selected the diazinedicarboxylate bridging ligands pyrazine-2,3- and -2,5-dicarboxylate (2,3- and 2,5-pyzdc) for our purpose. Here, we report the novel dimeric hybrid POM $[\mu\text{-}(2,3\text{-pyzdc})_2\{NaNi_2(H_2O)_4Sb_2W_{20}O_{70}\}_2]^{22-}$ (**Ni$_4$**) isolated as the salt $Na_{22}[\mathbf{Ni_4}]\cdot 85H_2O$ (**Na−Ni$_4$**).

The two pyzdc anions were systematically reacted in hot buffered NaOAc medium with four **M$_2$Sb$_2$** precursors (M = Mn, Co, Ni, Zn) following two different methods; one consists in the direct reaction between the ligand and the preformed **M$_2$Sb$_2$** precursor ($M_2Sb_2$:2L), whereas excess of ligand is added to **M$_2$Sb$_2$** generated in situ from the $[B\text{-}\alpha\text{-}SbW_9O_{33}]^{9-}$ species in the second method ($[SbW_9O_{33}]^{9-}$:$3M^{2+}$:2L). This results in 16 possible synthetic combinations, which were monitored by IR spectroscopy on any solid obtained by evaporation. Like in our previous work, the derivatization of Krebs-type POMs with bridging ligands proved to fully depend on the specific nature of the latter as only two out of the 16 combinations led to a hybrid species. The two pyzdc anions displayed remarkably different behavior. While 2,5-pyzdc showed to be inert (all solids obtained were simply **M$_2$Sb$_2$**), 2,3-pyzdc demonstrated selectivity toward **Ni$_2$Sb$_2$** regardless of the synthetic method, resulting in the isolation of **Na−Ni$_4$**. Unexpectedly, coordination of 2,3-pyzdc promoted a rearrangement of the Krebs-type framework into a significantly different cluster as indicated by the drastic modification of the POM domain when comparing the IR spectrum of **Na−Ni$_4$** to that of the **Ni$_2$Sb$_2$** precursor (Figure S1, Supporting Information, SI).

Single-crystal X-ray diffraction confirms the transformation of the **Ni$_2$Sb$_2$** skeleton upon coordination of 2,3-pyzdc. The hybrid

**Received:** November 5, 2014
**Published:** December 31, 2014





DOI: 10.1021/ic5026729
*Inorg. Chem.* 2015, 54, 409−411

**Ni$_4$** dimer is composed of two unprecedented {Na-Ni$_2$Sb$_2$W$_{20}$O$_{70}$} clusters (**Ni$_2$**) bridged by two 2,3-pyzdc ligands in ideal $C_2$ symmetry (Figure 1). Each **Ni$_2$** monomer is based on

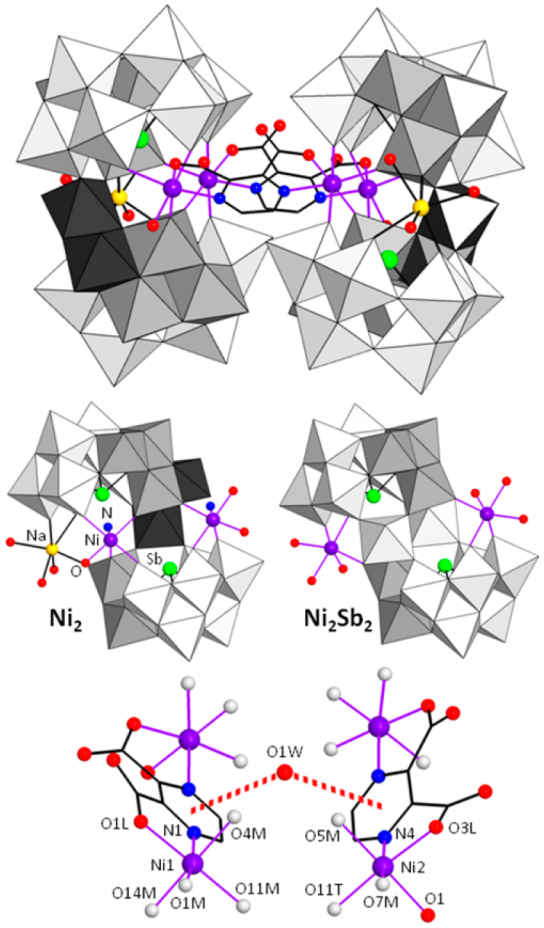


**Figure 1.** (Top) Structure of the **Ni$_4$** dimer (white for $WO_6$, gray for the 60°-rotated $\{W_3O_{13}\}$ trimer, dark gray for the $\{W_2O_{10}\}$ moiety). (Middle) Structural relationship between the **Ni$_2$** cluster and the **Ni$_2$Sb$_2$** precursor. (Bottom) Coordination sphere of the Ni atoms and detail of the nested $H_2O$ ($O_{POM}$, gray; $O_w$–H···$\pi$ interactions, dotted lines; selected bond lengths listed in Table S1, Supporting Information).

the novel 20-tungsto-2-antimonate(III) framework that can be rationalized as two trilacunary {B-$\beta$-SbW$_9$O$_{33}$} subunits linked by one edge-shared $\{W_2O_{10}\}$ moiety. The linking mode of this moiety is as follows: One W atom is incorporated in a trilacunary subunit by sharing edges with two octahedra of the 60°-rotated $\{W_3O_{13}\}$ trimer, while the other W atom is placed over the hexameric ring and shares a corner with a nonrotated trimer. The second subunit is then connected to this W atom via corner-sharing involving two trimers, including the rotated one. As a result of this insertion of a $\{W_2O_{10}\}$ moiety in a trilacunary subunit, the corresponding rotated trimer becomes a $\{W_5O_{20}\}$ fragment of edge-sharing octahedra that is closely related to the known $[HW_5O_{19}]^{7-}$ pentatungstate[7] (Figure S3, SI). Both contain a $\{W_4O_{16}\}$ rhombohedral core and differ in the position of the fifth $WO_6$, which is edge-shared to two octahedra and interacts with one internal O atom in $[HW_5O_{19}]^{7-}$, whereas it is connected to a single octahedron by sharing an external edge in $\{W_5O_{20}\}$. The $\{W_5O_{20}\}$ fragment in **Ni$_2$** has never been isolated as an independent species or as part of larger isopolytungstate aggregates to date.

The 20-tungsto-2-antimonate framework displays three coordination sites in its central belt. Two are occupied by Ni centers, and the third one is formally vacant but blocked by an octahedral $Na^+$ ion as observed for other 3d-metal-containing defect POMs.[8] The presence of coordinated Na ions appears to be a key factor in stabilizing the unprecedented **Ni$_2$** cluster found in **Na–Ni$_4$**. Both Ni centers display octahedral $NiO_5N$ chromophores. The coordination sphere of Ni1 is composed of the O,N atoms of a chelating 2,3-pyzdc ligand and two $O_{POM}$ atoms from each trilacunary unit that belong to adjacent rotated and nonrotated trimers. For Ni2, three $O_{POM}$ atoms occupy *fac*-related positions, two belonging to a $\{W_2O_{11}\}$ corner-shared fragment of one subunit and the remaining one to the rotated trimer of the other subunit. One water molecule (O1) and the O,N atoms of a second 2,3-pyzdc chelating ligand complete the coordination sphere. Thus, both 2,3-pyzdc anions display bridging bis(bidentate) coordination modes with the carboxylate groups slightly tilted with respect to the pyz ring as a result of steric hindrance (dihedral angles of 15 and 31°). Noncoplanar configurations are not unusual for this ligand.[9] Moreover, the two pyz rings are tilted 40° out of the plane defined by the Ni atoms and this creates a central aromatic nest where a water molecule (O1W) is hosted via nonconventional $O_w$–H···$\pi$ hydrogen bonds (Figure 1). The distance of O1W to the ring centroids (3.217(2) Å) compares well to that calculated for the hydrogen-donor/acceptor water/benzene system and to those observed experimentally.[10]

The structure of **Ni$_2$** is closely related to that of **Ni$_2$Sb$_2$**,[5c] and it is likely formed upon a skeletal rearrangement promoted by coordination of the 2,3-pyzdc ligands. Compared to the parent POM, a **Ni$_2$** cluster would show a trilacunary unit incorporating an additional $WO_6$ in the 60°-rotated trimer via edge-sharing and one $\{Ni(H_2O)_2\}$ and one $\{Na(H_2O)_3\}$ moieties in place of one internal ($WO_2$) and one external $\{Ni(H_2O)_3\}$ groups (Figure 1). Therefore, **Ni$_2$** could be seen as the product of the migration of a belt-($WO_2$) group toward the cleft between a rotated $\{W_3O_{13}\}$ trimer and the second ($WO_2$) moiety. A Ni atom would consequently replace the migrated group at the internal site in the POM belt, which would in turn leave a formally vacant external position that is blocked by the incorporation of a Na ion to stabilize the resulting assembly.

To explore the solution behavior of the dimeric **Ni$_4$** anion, ESI-MS studies were carried out (Figure S4, SI). The negative ESI mass spectrum of an aqueous solution of **Na–Ni$_4$** shows three groups of signals, which are due to monomeric species of similar composition and charge states of 5–, 4–, and 3–, according to the isotopic pattern inspection and the $m/z$ spacing. These monomers are best described as pristine **Ni$_2$** clusters, and hence, the most abundant group of signals centered at $m/z$ 1043.7 must correspond to the series of anions $[Ni_2Sb_2W_{20}O_{70} + xH_2O + mH^+ + (5-m)Na^+]^{5-}$ ($\{$**Ni$_2$**$\}^{5-}$), while the groups at $m/z$ 1310.7 and 1751.0 are readily assigned to the series $[Ni_2Sb_2W_{20}O_{70} + xH_2O + mH^+ + (6-m)Na^+]^{4-}$ ($\{$**Ni$_2$**$\}^{4-}$) and $[Ni_2Sb_2W_{20}O_{70} + xH_2O + mH^+ + (7-m)Na^+]^{3-}$ ($\{$**Ni$_2$**$\}^{3-}$), respectively. The different extent of protonation, counterion content and associated water molecules displayed by the gas-phase detected species is common to highly charged POMs like **Ni$_2$**.[11] Combined $^1$H/DOSY NMR experiments confirm that release of the 2,3-pyzdc ligands and consequent fragmentation of **Ni$_4$** takes place upon dissolution rather than being induced by the ionization process (SI). The above, together with a lack of signals originating from any oligomer, shows that the **Ni$_4$** dimer fully dissociates into pristine **Ni$_2$** monomers in water. However, this


DOI: 10.1021/ic5026729
*Inorg. Chem.* 2015, 54, 409–411

might be hindered to some extent by the presence of organic solvents as evidenced by analogous ESI-MS experiments using water:acetone (1:4) mixtures. In this case, four additional groups of signals were observed in the $m/z$ 1550−3100 region that are attributed to intact **Ni$_4$** dimers detected as the corresponding series of anions with charge states ranging from 7− to 4−.

The $\chi_m T$ product of **Na−Ni$_4$** at room temperature is 5.065 cm$^3$ K mol$^{-1}$ (Figure S5, SI), in good agreement with that expected for four noninteracting octahedral Ni$^{II}$ ions (5.068 cm$^3$ K mol$^{-1}$, $S = 1$, $g = 2.25$). The $\chi_m T$ curve remains nearly constant down to about 30 K, below which it undergoes a drastic decrease to reach a value of 4.15 cm$^3$ K mol$^{-1}$ at 5 K. Curie−Weiss behavior is observed for nearly the whole temperature range analyzed ($C_m$ = 5.07 cm$^3$ K mol$^{-1}$, $\theta$ = −0.4 K). The negative value of $\theta$ and decrease in $\chi_m T$ below 30 K could be indicative of weak antiferromagnetism (AF). It is known that O−W−O pathways lead to negligible exchange between paramagnetic centers,[12] and hence, **Ni$_4$** could be magnetically described as two isolated {Ni$_2$($\mu$-2,3-pyzdc)} dimers with a Ni···Ni distance of 6.807(4) Å because the two Ni$^{II}$ centers on each **Ni$_2$** half are connected by one {WO$_6$} and one {W$_2$O$_{10}$} fragments. Following this assumption, susceptibility data were fitted using eq 1 (SI), which corresponds to a $S = 1$ dimer but expressed per metal atom and multiplied by the four Ni$^{2+}$ ions in **Ni$_4$**.[13] The best fit results afford an intradimeric exchange coupling constant of $J$ = −0.35 cm$^{-1}$ ($g = 2.25$, $H = -2JS_1S_2$). This value is comparable to that calculated for the [Ni(2,3-pyzdc)(H$_2$O)$_2$] chain with extremely weak AF behavior,[9a] but the model does not reproduce the $\chi_m T$ curve satisfactorily below about 130 K. We then assumed the zero-field splitting (ZFS) effect to be operative in our system and fitted the experimental data to eq 2 (SI), which considers four isolated $S = 1$ atoms showing single ion ZFS.[14] The whole $\chi_m T$ curve is very well reproduced with this model, and the best fit results afford a ZFS value of $D$ = 6.5 cm$^{-1}$ ($g = 2.25$). This shows that the magnetic behavior of **Na−Ni$_4$** is dominated by the single ion anisotropy rather than by any isotropic magnetic exchange.

This work illustrates how novel frameworks might be obtained through skeletal rearrangement of POM assemblies with exposed metal centers upon ligand attack. In our case, selective coordination of 2,3-pyzdc to the **Ni$_2$Sb$_2$** Krebs POM led to [(2,3-pyzdc)$_2${NaNi$_2$(H$_2$O)$_4$Sb$_2$W$_{20}$O$_{70}$}$_2$]$^{22-}$(**Ni$_4$**) composed of two unprecedented dinickel containing 20-tungsto-2-antimonate(III) clusters linked by N,O-bis(bidentate) bridging ligands. This dimeric assembly undergoes full or partial dissociation upon dissolution in water or water:acetone (1:4) mixtures, respectively, and its magnetic properties are dominated by zero-field splitting of the Ni$^{II}$ centers. The enormous variety of bridging ligands available will allow us to thoroughly extend these systematic studies in quest of novel POM architectures. Moreover, **Ni$_4$** can be seen as a defect 3d-metal-containing POM with one Na-blocked vacant site, and hence, it could be a good candidate for incorporating additional electrophiles.

## ■ ASSOCIATED CONTENT

### Supporting Information

Experimental section, IR and ESI-MS spectra, TGA/DTA curves, structural figures, magnetic curves and equations, and X-ray crystallographic data in CIF format. This material is available free of charge via the Internet at http://pubs.acs.org.

## ■ AUTHOR INFORMATION

### Corresponding Authors

*E-mail: santiago.reinoso@ehu.es.

*E-mail: juanma.zorrilla@ehu.es.

### Notes

The authors declare no competing financial interest.

## ■ ACKNOWLEDGMENTS

Financial support: EJ/GV (S-PE13UN056, IT477-10, and predoctoral fellowship to B.A.), MINECO (MAT2013-48366-C2-2-P), and UPV/EHU (UFI11/53). Technical and human support: SGIker (UPV/EHU) and SCIC (UJI).

## ■ REFERENCES

(1) (a) Pope, M. T. *Heteropoly and Isopoly Oxometalates*; Springer-Verlag: Berlin, Germany, 1983. (b) *Polyoxometalate Chemistry for Nanocomposite Design*; Pope, M. T., Yamase, T., Eds.; Kluwer: Dordrecht, The Netherlands, 2002.

(2) (a) Proust, A.; Thouvenot, R.; Gouzerh, P. *Chem. Commun.* **2008**, 1837−1852. (b) Dolbecq, A.; Dumas, E.; Mayer, C. R.; Mialane, P. *Chem. Rev.* **2010**, *110*, 6009−6048. (c) Proust, A.; Matt, B.; Villanneau, R.; Guillemot, G.; Gouzerh, P.; Izzet, G. *Chem. Soc. Rev.* **2012**, *41*, 7605−7622.

(3) (a) Peng, Z. *Angew. Chem., Int. Ed.* **2004**, *43*, 930−935. (b) Boglio, C.; Micoine, K.; Derat, E.; Thouvenot, R.; Hasenknopf, B.; Thorimbert, S.; Lacôte, E.; Malacria, M. *J. Am. Chem. Soc.* **2008**, *130*, 4553−4561. (c) Nomiya, K.; Togashi, Y.; Kasahara, Y.; Aoki, S.; Seki, H.; Noguchi, M.; Yoshida, S. *Inorg. Chem.* **2011**, *50*, 9606−9619. (d) Villanneau, R.; Racimor, D.; Messner-Henning, E.; Rousselière, H.; Picart, S.; Thouvenot, R.; Proust, A. *Inorg. Chem.* **2011**, *50*, 1164−1166. (e) Tong, U. S.; Chen, W.; Ritchie, C.; Wang, X.; Song, Y.-F. *Chem.—Eur. J.* **2014**, *20*, 1500−1504.

(4) (a) Mialane, P.; Dolbecq, A.; Sécheresse, F. *Chem. Commun.* **2006**, 3477−3485. (b) Fang, X.; Anderson, T. M.; Hill, C. L. *Angew. Chem., Int. Ed.* **2005**, *44*, 3540−3544. (c) Zheng, S.-T.; Zhang, J.; Yang, G.-Y. *Angew. Chem., Int. Ed.* **2008**, *47*, 3909−3913. (d) Rousseau, G.; Oms, O.; Dolbecq, A.; Marrot, J.; Mialane, P. *Inorg. Chem.* **2011**, *50*, 7376−7378.

(5) (a) Loose, I.; Droste, E.; Bösing, M.; Pohlmann, H.; Dickman, M. H.; Rosu, C.; Pope, M. T.; Krebs, B. *Inorg. Chem.* **1999**, *38*, 2688−2694. (b) Piepenbrink, M.; Limanski, E. M.; Krebs, B. *Z. Anorg. Allg. Chem.* **2002**, *628*, 1187−1191. (c) Liu, Y.-H.; Ma, P.-T.; Wang, J.-P. *J. Coord. Chem.* **2008**, *61*, 936−944.

(6) Artetxe, B.; Reinoso, S.; San Felices, L.; Vitoria, P.; Pache, A.; Martín-Caballero, J.; Gutiérrez-Zorrilla, J. M. *Inorg. Chem.* **2014**, DOI: 10.1021/ic502232v.

(7) Fuchs, J.; Palm, R.; Hartl, H. *Angew. Chem., Int. Ed. Engl.* **1996**, *35*, 2651−2653.

(8) (a) Kortz, U.; Mbomekalle, I. M.; Keita, B.; Nadjo, L.; Berthet, P. *Inorg. Chem.* **2002**, *41*, 6412−6416. (b) Ruhlmann, L.; Canny, J.; Contant, R.; Thouvenot, R. *Inorg. Chem.* **2002**, *41*, 3811−3819.

(9) (a) Mao, L.; Rettig, S. J.; Thompson, R. C.; Trotter, J.; Xia, S. *Can. J. Chem.* **1996**, *74*, 433−444. (b) Beobide, G.; Castillo, O.; García-Couceiro, U.; García-Terán, J. P.; Román, P. *Inorg. Chem.* **2006**, *45*, 5367−5382.

(10) (a) Steiner, T.; Schreurs, A. M. M.; Kanters, J. A.; Kroon, J. *Acta Crystallogr.* **1998**, *D54*, 25−31. (b) Jorgensen, W. L.; Severance, D. L. *J. Am. Chem. Soc.* **1990**, *112*, 4768−4774. (c) Callejo, L. M.; Muga, I.; Vitoria, P.; Reinoso, S.; Román, P.; Gutiérrez-Zorrilla, J. M. *Acta Crystallogr.* **2003**, *E59*, m684−m686.

(11) Miras, H. N.; Zang, H. Y.; Long, D.-L.; Cronin, L. *Eur. J. Inorg. Chem.* **2011**, 5105−5111.

(12) Kortz, U.; Nellutla, S.; Stowe, A. C.; Dalal, N. S.; van Tol, J.; Bassil, B. S. *Inorg. Chem.* **2004**, *43*, 144−154.

(13) Santana, M. D.; García, G.; Vicente-Hernández, C.; García, L.; Pérez, J.; Rojo, T.; Lezama, L. *J. Organomet. Chem.* **2008**, *693*, 2009−2016.

(14) López-Banet, L.; Santana, M. D.; García, G.; García, L.; Pérez, J.; Rojo, T.; Lezama, L.; Costes, J. P. *Inorg. Chem.* **2011**, *50*, 437−443.



DOI: 10.1021/ic5026729
*Inorg. Chem.* 2015, 54, 409−411